Journal of Molecular Catalysis B: Enzymatic 69 (2011) 89–94

Contents lists available at ScienceDirect

Journal of Molecular Catalysis B: Enzymatic

journal homepage: www.elsevier.com/locate/molcatb

Kinetic mechanism of 3-ketoacyl-(acyl-carrier-protein) reductase from *Synechococcus* sp. strain PCC 7942: A useful enzyme for the production of chiral alcohols

Kathrin Hölsch, Dirk Weuster-Botz*

Lehrstuhl für Bioverfahrenstechnik, Technische Universität München, Boltzmannstr. 15, 85748 Garching, Germany

ARTICLE INFO

Article history:
Received 9 September 2010
Received in revised form
16 December 2010
Accepted 27 December 2010
Available online 7 January 2011

Keywords:
Chiral alcohols
Enzyme kinetics
Oxidoreductase
SDR superfamily
Steady-state ordered Bi Bi mechanism

ABSTRACT

Mathematical models and simulations have become indispensable tools for the characterization and optimization of enzymatic processes. Nonetheless, industrially relevant enzymes are often poorly characterized with respect to enzyme kinetics. For the description of bisubstrate reactions catalysed by oxidoreductases in many cases Michaelis–Menten kinetics is used, which is a significant simplification. The NADPH-dependent 3-ketoacyl-(acyl-carrier-protein) reductase (KR) from *Synechococcus* sp. strain PCC 7942 is an interesting biocatalyst for the asymmetric synthesis of a variety of chiral building blocks, such as ethyl (*S*)-4-chloro-3-hydroxybutanoate. Initial-rate analysis of the KR-catalysed reduction of ethyl 4-chloroacetoacetate to the corresponding (*S*)-alcohol gave families of straight lines in double-reciprocal plots consistent with a sequential mechanism being obeyed. Product inhibition studies revealed that the KR follows a steady-state ordered Bi Bi mechanism with NADPH binding first. This result was corroborated by fluorescence enhancement studies, which indicated that the cofactor can bind to the free enzyme. The dissociation constants for the binary NADPH–protein complex determined kinetically and by fluorescence titration were identical within experimental error (1.04 ± 0.35 mM and 1.01 ± 0.23 mM) and confirmed the accuracy of the obtained kinetic parameters.

1. Introduction

Mechanistic kinetic models have been shown to be valuable tools for the optimization of various kinds of enzymatic reactions (e.g. [1–3]). Prerequisites for the accurate modelling of biocatalytic processes are the detailed knowledge of the kinetic mechanism and the determination of the kinetic parameters of all enzymes that are involved.

Oxidoreductases are important biocatalysts for the industrial production of chiral building blocks [4,5]. The asymmetric synthesis of chiral alcohols catalysed by oxidoreductases is a classical "Bi Bi" reaction involving two substrates and two products: a keto compound and a reduced cofactor, mostly NADH or NADPH, are converted to the corresponding hydroxy compound and the oxidized cofactor. The rate equations for bisubstrate mechanisms are more complex than the Michaelis–Menten model, which is used to describe monosubstrate reactions. In a simplifying approach, Michaelis–Menten kinetics can also be applied to bisubstrate reactions if pseudo-first-order reaction conditions are achieved and the concentration of one of the substrates is kept at a constant, saturating surplus ($\geq 10 \times K_m$). However, this assumption is not valid for the whole time course of preparative enzymatic reactions involving oxidoreductases, because the nicotinamide cofactors are expensive and are therefore not provided in excess quantities. Quite the contrary, cost-effective industrial bioreductions rely on efficient *in situ* regeneration of catalytic amounts of reduced cofactors [6,7]. For these reasons, the determination of the kinetic mechanism and the subsequent development of a detailed mathematical model that allows for the prediction of the enzymatic activity as function of concentrations of substrates, cofactors and inhibiting compounds are essential for process optimizations.

Ethyl (*S*)-4-chloro-3-hydroxybutanoate ((*S*)-ECHB) is a key intermediate in the synthesis of 3-hydroxy-3-methylglutaryl coenzyme A (HMG-CoA) reductase inhibitors, also known as statins [8]. This important chiral building block can be easily obtained by asymmetric bioreduction of the prochiral β-keto ester ethyl 4-chloroacetoacetate (ECAA). A kind of oxidoreductase that has recently attracted attention due to the ability to reduce ECAA to the corresponding (*S*)-alcohol (Scheme 1A) is the fatty acid biosynthetic enzyme 3-ketoacyl-[acyl-carrier-protein (ACP)] reductase (KR, EC 1.1.1.100) [9–11]. This enzyme belongs to the dissociated

Abbreviations: ACP, acyl carrier protein; ECAA, ethyl 4-chloroacetoacetate; ECHB, ethyl 4-chloro-3-hydroxybutyrate; KR, 3-ketoacyl-(acyl-carrier-protein) reductase; SDR, short-chain dehydrogenase/reductase.

* Corresponding author. Tel.: +49 089 28915713; fax: +49 089 28915714.
E-mail address: D.Weuster-Botz@lrz.tum.de (D. Weuster-Botz).

1381-1177/$ – see front matter © 2011 Published by Elsevier B.V.
doi:10.1016/j.molcatb.2010.12.013

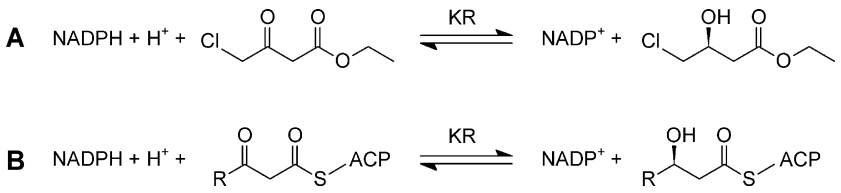

Scheme 1. Reactions catalysed by 3-ketoacyl-[acyl-carrier-protein (ACP)] reductase (KR). (A) Reduction of ethyl 4-chloroacetoacetate. (B) Reduction of 3-ketoacyl-ACP. R denotes the growing acyl chain.

type II fatty acid synthase (FAS II) system occurring in plants and most bacteria [12] and is a member of the short-chain dehydrogenase/reductase (SDR) superfamily. Its physiological function is the reduction of 3-ketoacyl-ACP to (*R*)-3-hydroxyacyl-ACP with NADPH as cofactor (Scheme 1B) [13,14].

The enzymatic activities and enantiomeric excesses observed in biocatalytic reductions of ECAA using KRs from different organisms ranged between 0.1 and 250 U mg^{-1} and 53.4 to >99.8% (*S*), respectively [9,11]. Enantiomeric excesses higher than 99% were only reported for enzymes originating from cyanobacteria [11], because of which they are especially attractive for preparative applications. Thus, more information about the kinetics of the enzymatic reaction catalysed by cyanobacterial KRs would be valuable.

Since KRs are regarded as promising targets for the development of antimicrobial agents [15], the kinetic mechanisms of enzymes from several pathogenic microorganisms, such as *Streptococcus pneumoniae* and *Plasmodium falciparum*, have been determined [16–19]. The type of bisubstrate mechanism varied between ordered Bi Bi and random Bi Bi reactions among KRs from different species. This points to the fact that enzymes from different sources have evolved to catalyse the same reaction through different mechanisms. Here, we present the first determination of the kinetic mechanism from a KR originating from the large phylum of cyanobacteria. For this study, the KR from the freshwater cyanobacterium *Synechococcus* sp. strain PCC 7942 was chosen because it is the best studied cyanobacterial KR so far [10,11].

2. Materials and methods

2.1. Chemicals

Ethyl 4-chloroacetoacetate (ECAA) (>98.0%) was purchased from Merck (Darmstadt, Germany). Ethyl (*S*)-4-chloro-3-hydroxybutyrate ((*S*)-ECHB) (~96.0%) and ethyl (*R*)-4-chloro-3-hydroxybutyrate ((*R*)-ECHB) (98.0%) were obtained from Sigma–Aldrich (Schnelldorf, Germany). The cofactors NADP-Na (>95.0%) and NADPH-Na_4 (>97.0%) were bought from Calbiochem (part of Merck, Darmstadt, Germany) and Carl Roth (Karlsruhe, Germany), respectively. All other chemicals were of analytical grade from various suppliers.

2.2. Cloning, expression and purification

The KR from *Synechococcus* sp. strain PCC 7942 was cloned, heterologously expressed in *Escherichia coli* (*E. coli*) and purified as described previously [10]. The homogeneity of the protein preparation was analysed by 15% Tris–glycine SDS-PAGE stained with silver according to the method by Heukeshofen and Dernik [20]. Since no contaminating protein was detected in the KR preparation, the purity was judged to be near 100%.

2.3. Enzyme assays

All assays for KR activity were performed in 0.1 M sodium phosphate buffer (pH 7.0) at 30 °C in a reaction volume of 200 μL. The assay mixtures contained 0–37.5 mM ECAA and 0–4 mM NADPH. Controls lacking enzyme were routinely included. The samples used for the determination of product inhibition patterns contained 0–16 mM $NADP^+$ and 0–50 mM (*S*)-ECHB, respectively. All samples were preincubated for 5 min before the reaction was initiated by the addition of β-keto ester. Protein concentrations were determined with the bicinchoninic acid (BCA) assay (Pierce, Rockford, USA) and ranged from 10 to 50 mg L^{-1}. Under these conditions, the enzyme activity was proportional to the KR concentration. One unit (U) corresponds to the amount of enzyme converting 1 μmol substrate per min at 30 °C. The oxidation of NADPH was measured photometrically at 340 nm in microtiterplates. The reduction of β-keto esters was measured by chiral gas chromatography. For this purpose, enzyme reactions were carried out in 1.5 mL safe lock tubes using a heating shaker (Eppendorf, Hamburg, Germany) at 600 rpm. The reactions were stopped by adding ethyl acetate (−20 °C) at a volume ratio of 1:1 and the samples were immediately placed in an ice chest. The extraction of substrates and products was performed using a mixer mill (Retsch, Haan, Germany) for 10 min at 30 Hz.

2.4. Gas chromatographic analysis

A Varian CP-3800 gas chromatograph (GC) equipped with a Flame Ionization Detector (FID) and a Lipodex-E (25 m × 0.25 mm ID) column (Macharey-Nagel, Düren, Germany) was used for analysis of β-keto and β-hydroxy esters. The helium flow rate was maintained at 4 mL min^{-1}. Chiral analysis of ECAA, (*R*)- and (*S*)-ECHB was performed as described by Bräutigam et al. [21].

2.5. Data analysis

Initial half saturation constants for ECAA and NADPH were determined by varying the concentration of the substrate while maintaining the cofactor NADPH at a fixed saturating level ($\geq 10 \times K_m$ (app)) and vice versa [10]. Enzyme activities were measured under initial reaction rate conditions in triplicates. Subsequently, the data were fitted to the Michaelis–Menten equation (Eq. (1)):

$$v = \frac{V_{max}[S]}{K_m(app) + [S]} \quad (1)$$

where v is the reaction rate, V_{max} is the maximum reaction rate, [S] is the substrate concentration and K_m (app) is the apparent half-saturation constant.

To investigate further the kinetic mechanism and the order of substrate binding, assays were performed where each substrate was varied in turn with a fixed concentration of one of the products, either $NADP^+$ or β-hydroxy ester. The second substrate was kept constant at a sub-saturating concentration. The pattern of the corresponding double-reciprocal plot was analysed and assigned as linear competitive (Eq. (2)), uncompetitive (Eq. (3)), or non-competitive/mixed (Eq. (4)) inhibition:

$$v = \frac{V_{max}[S]}{K_m(1 + ([I]/K_{ic})) + [S]} \quad (2)$$

$$v = \frac{V_{max}[S]}{K_m + [S](1 + ([I]/K_{iu}))} \quad (3)$$

$$v = \frac{V_{max}[S]}{K_m(1 + ([I]/K_{ic})) + [S](1 + ([I]/K_{iu}))} \quad (4)$$

where K_{ic} is the inhibitor dissociation constant of the enzyme–inhibitor complex and K_{iu} is the inhibitor dissociation constant of the enzyme–substrate–inhibitor complex. All kinetic model parameters were identified by nonlinear regression analysis using the software program SigmaPlot 8.0 (SYSTAT Software, Point Richmond, CA).

2.6. Determination of the NADPH dissociation constant

The dissociation constant of NADPH (K_d) was determined by fluorescence titration using a Tecan Infinite M200 reader (Tecan, Männedorf, Switzerland). The fluorescence was excited at 280 nm in the presence of increasing NADPH concentrations (0–1.04 mM) in 0.1 M phosphate buffer (pH 7.0) at a protein concentration of 1.29 μM. The dilution was kept below 5% and the fluorescence emitted at 450 nm was measured. A control titration was carried out in which the fluorescence of NADPH added in 1 μL-aliquots to the buffer solution was determined. All data were corrected for dilution, fluorescence of enzyme and buffer, and inner filter effects [22]:

$$F_c = F \cdot 10^{(A_{ex}+A_{em})/2} \quad (5)$$

where F_c is the corrected intensity, F the measured intensity, and A_{ex} and A_{em} are the absorbances of the sample at the excitation and emission wavelength, respectively.

NADPH binding resulted in an enhanced fluorescence emission at 450 nm due to energy transfer from tryptophan to NADPH. The difference between the fluorescence measured in the presence of the protein and the fluorescence of the control (ΔF_c) was calculated, which correlates with the amount of bound NADPH. The dissociation constant K_d was determined by plotting the change in emission against the free NADPH concentration. The SigmaPlot 8.0 software was used to fit the data to Eq. (6) by nonlinear regression:

$$\Delta F_c = \Delta F_{c\,max} \cdot \frac{[NADPH_{free}]}{K_d + [NADPH_{free}]} \quad (6)$$

Because a significant part of the added cofactor could have been bound to the enzyme, the concentration of free NADPH was calculated as follows [23]:

$$\frac{\Delta F_c}{\Delta F_{c\,max}} = \frac{[KR_{bound}]}{[KR_{total}]} \quad (7)$$

$$[KR_{bound}] = [NADPH_{bound}] \quad (8)$$

$$[NADPH_{free}] = [NADPH_{total}] - [NADPH_{bound}] \quad (9)$$

At each cofactor concentration, only a negligible percentage (≤0.2%) of the total NADPH was enzyme-bound.

3. Results

3.1. Initial reaction rate studies

As a first step in the determination of the kinetic mechanism, the reaction rate with ECAA was measured at several fixed concentrations of NADPH. The double-reciprocal plots of initial reaction rate against ECAA concentration yielded a family of straight lines intersecting to the left of the ordinate (Fig. 1). Replots of the slopes and intercepts against the reciprocal of the fixed substrate concentration were also linear (Fig. 1 inset). When the concentration of NADPH was varied and the ECAA concentration was kept constant, the double reciprocal plots gave the same pattern of lines intersecting in the second quadrant (data not shown). These results are indicative of a sequential mechanism in which both substrates are added to the enzyme before a product is released and rule out the possibility of a ping-pong mechanism, which yields parallel lines in a double-reciprocal plot. Moreover, the results are incompatible with a rapid-equilibrium ordered mechanism because an intersection point on the y-axis would have been expected for one of the substrates [24].

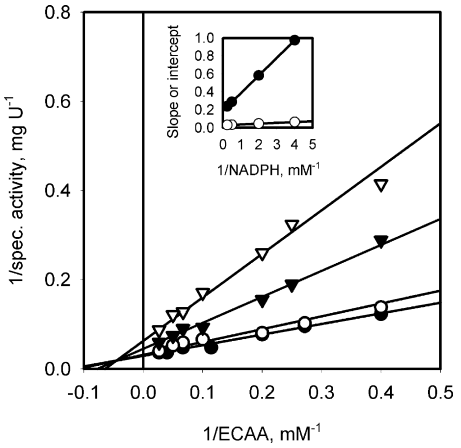

Fig. 1. Initial reaction rate pattern. Double-reciprocal plots of reaction rates with ECAA as variable substrate at four concentrations of NADPH are shown. The fixed NADPH concentrations were 0.25 mM (▽), 0.5 mM (▼), 2 mM (○), and 4 mM (●). The inset shows replots of slopes (●) and intercepts (○) versus the reciprocal concentration of the fixed substrate.

3.2. Product inhibition studies

To distinguish between different sequential bisubstrate mechanisms, a product inhibition analysis under non-saturating conditions was performed. The products of the reaction catalysed by the KR were applied as inhibitors of the forward reaction (Fig. 2). For the definition of non-saturating conditions, apparent half-saturation constants were used (K_m (app) NADPH: 0.40 ± 0.03 mM; K_m (app) ECAA: 8.3 ± 1.2 mM). Since the enantiomeric excess of (*S*)-ECHB was determined to be 99.8 ± 0.4%, only the (*S*)-alcohol was examined as inhibitor [10].

The double-reciprocal plots of the results showed that $NADP^+$ was a linear competitive inhibitor with respect to NADPH (Fig. 2A), but was a mixed inhibitor with respect to ECAA (Fig. 2C). In contrast, (*S*)-ECHB was a mixed inhibitor of both NADPH (Fig. 2B) and ECAA (Fig. 2D). All replots of slopes and intercepts from product inhibition studies were linear. The inhibition patterns and kinetic parameters are summarized in Table 1.

Taken together, the initial reaction rate and product inhibition patterns are consistent with a steady-state ordered Bi Bi mechanism with NADPH binding first, which is described in Eq. (10) [24]:

$$v = \frac{V_1V_2([A][B] - ([P][Q])/K_g)}{K_{iA}K_{mB}V_2 + K_{mB}V_2[A] + K_{mA}V_2[B] + (K_{mQ}V_1[P])/K_g + (K_{mP}V_1[Q])/K_g + V_2[A][B] + (K_{mQ}V_1[A][P])/K_{iA}K_g + (K_{mA}V_2[B][Q])/K_{iQ} + (V_1[P][Q])/K_g + (V_2[A][B][P])/K_{iP} + (V_1[B][P][Q])/K_{iB}K_g} \quad (10)$$

where V_1 and V_2 are the maximum reaction rates of the forward and the reverse reaction, [A], [B], [P] and [Q] represent the concentrations of NADPH, ECAA, (*S*)-CHBE and $NADP^+$, K_{mA}, K_{mB}, K_{mP}, K_{mQ} and K_{iA}, K_{iB}, K_{iP}, K_{iQ} are the respective half-saturation and

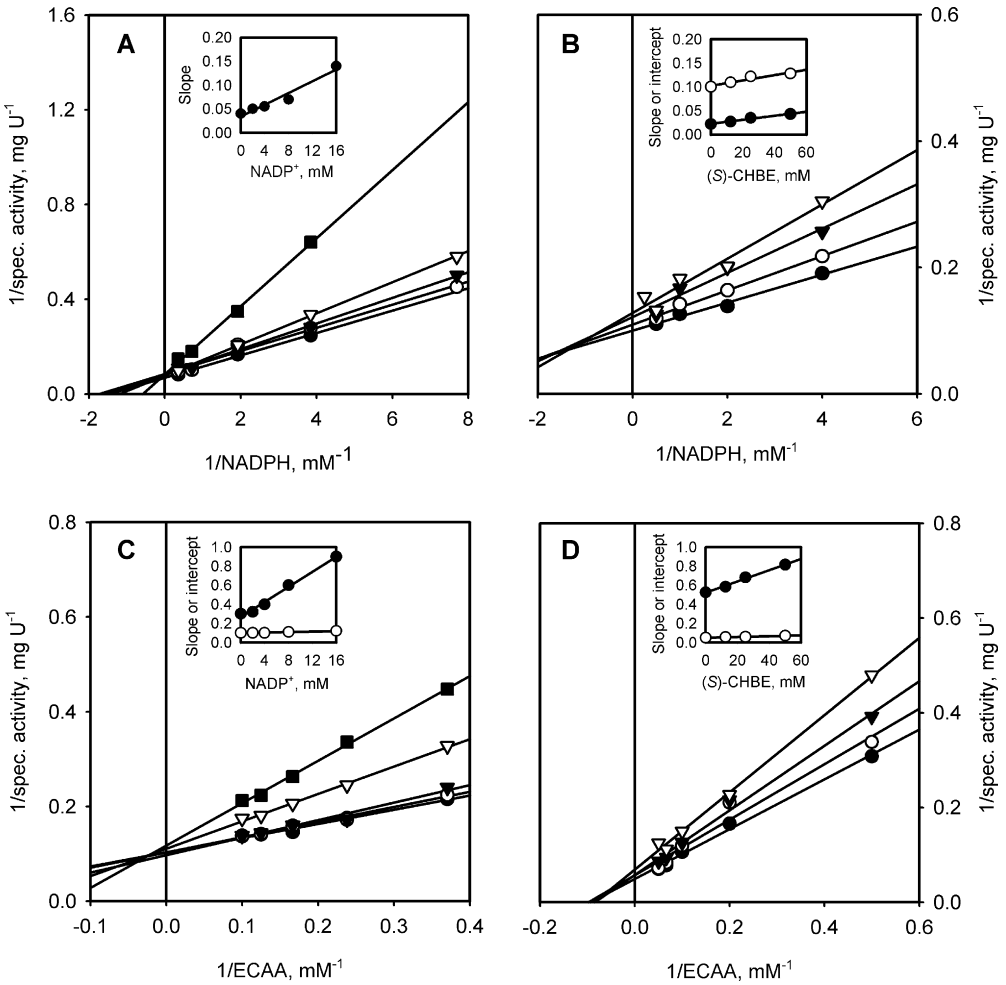

Fig. 2. Product inhibition studies under non-saturating conditions. The kinetic data are displayed as double reciprocal plots of the reaction rate versus substrate concentrations at different concentrations of the product inhibitor. For each plot, one substrate was kept at a constant non-saturating level while the second substrate and the product inhibitor concentrations were varied. (A) $NADP^+$ is a competitive inhibitor to NADPH. ECAA was kept constant at 4 mM while varying NADPH and $NADP^+$ concentrations (● = 0, ○ = 2, ▼ = 4, ▽ = 8, ■ = 16 mM). (B) (*S*)-ECHB is a mixed-type inhibitor to NADPH. ECAA was kept constant at 4 mM while varying NADPH and (*S*)-ECHB concentrations (● = 0, ○ = 12.5, ▼ = 25, ▽ = 50 mM). (C) $NADP^+$ is a mixed-type inhibitor to ECAA. NADPH was kept constant at 0.4 mM while varying ECAA and $NADP^+$ concentrations (● = 0, ○ = 2, ▼ = 4, ▽ = 8, ■ = 16 mM). (D) (*S*)-ECHB is a mixed-type inhibitor to ECAA. NADPH was kept constant at 0.5 mM while varying ECAA and (*S*)-ECHB concentrations (● = 0, ○ = 12.5, ▼ = 25, ▽ = 50 mM). The insets show replots of slopes (●) and intercepts (○) versus inhibitor concentrations.

dissociation constants, and K_g is the equilibrium constant of the reaction. Under initial reaction rate conditions, this equation reduces to

$$v = \frac{V_1[A][B]}{K_{iA}K_{mB} + K_{mB}[A] + K_{mA}[B] + [A][B]} \quad (11)$$

for the forward reaction and

$$v = \frac{V_2[P][Q]}{K_{iA}K_{mB} + K_{mQ}[P] + K_{mP}[Q] + [P][Q]} \quad (12)$$

for the reverse reaction.

As the very low rate of the reverse reaction precluded detailed kinetic analyses, it was not possible to identify all of the kinetic model parameters. The maximum reaction rate of the reverse reaction was estimated to be 0.15 U mg^{-1}, which equals about 0.4% of the maximum reaction rate of the forward reaction. Because both products of the reverse reaction, ECAA and NADPH, have only limited stability under the assay conditions [25,26], long incubation times were incompatible with accurate results. Therefore, kinetic studies of the reverse reaction were not pursued further.

The kinetic data obtained for the forward reaction in the absence of products were globally fitted to the equation for the steady-state ordered Bi Bi mechanism (Eq. (11)) (Fig. 3). The derived kinetic constants are: $V_1 = 36.79 \pm 2.11$ U mg^{-1}, K_{mA} (NADPH) = 0.33 ± 0.9 mM, K_{mB} (ECAA) = 6.94 ± 1.34 mM, and K_{iA} = 1.04 ± 0.35 mM.

Table 1
Product inhibition patterns and derived inhibition constants.

Varied substrate	Product (inhibitor)	Inhibition pattern	Inhibition constant	
			K_{ic} (mM)	K_{iu} (mM)
NADPH	$NADP^+$	Competitive	6 ± 1	–
NADPH	(*S*)-ECHB	Mixed (non-competitive)	47 ± 20	210 ± 98
ECAA	$NADP^+$	Mixed (non-competitive)	8 ± 3	68 ± 59
ECAA	(*S*)-ECHB	Mixed (non-competitive)	94 ± 54	115 ± 71

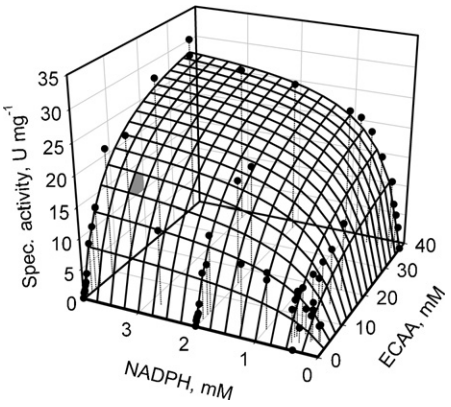

Fig. 3. Graphical representation of the initial reaction rate data obtained in the absence of products. The experimental data are shown as dots and the lines represent the predicted values obtained by fitting the data points to Eq. (11) by nonlinear regression analysis.

3.3. NADPH binding studies

Interaction between the free enzyme and NADPH was further demonstrated by the transfer of energy between the protein and the cofactor. Excitation of tryptophan fluorescence at 280 nm in the presence of increasing NADPH concentrations caused the cofactor to emit an increasing amount of light at 450 nm and gave evidence of the formation of a binary enzyme-cofactor complex (Fig. 4). Because NADPH concentrations higher than 1.04 mM exceeded the absorbance measurement range of the photometer, the fluorescence values measured at these concentrations could not be corrected for inner filter effects and were not used for the determination of the dissociation constant K_d of the enzyme-NADPH complex. Nonlinear regression analysis of the data yielded a dissociation constant K_d of 1.01 ± 0.23 mM. This result is in good agreement with the parameter K_{iA} (1.04 ± 0.35 mM) of the ordered Bi Bi mechanism, which represents the dissociation constant of the first substrate to bind to the free enzyme.

4. Discussion

The results from the initial reaction rate, product inhibition, and NADPH-binding studies led to the conclusion that the KR from the freshwater cyanobacterium *Synechococcus* sp. strain PCC 7942 operates by a steady-state ordered Bi Bi mechanism involving a ternary complex with NADPH binding before the keto substrate. The estimated maximum reaction rate of the forward reaction (36.79 ± 2.11 U mg^{-1}) is not significantly different from the specific activity of the KR that was determined in previous experiments with ECAA and NADPH in excess (38.29 ± 2.15 U mg^{-1}) [10]. The consistencies of these independently determined parameters and of the dissociation constants of the binary NADPH–protein complex determined via kinetic experiments (1.04 ± 0.35 mM) and fluorescence enhancement (1.01 ± 0.23 mM) verify the correctness of the obtained kinetic model.

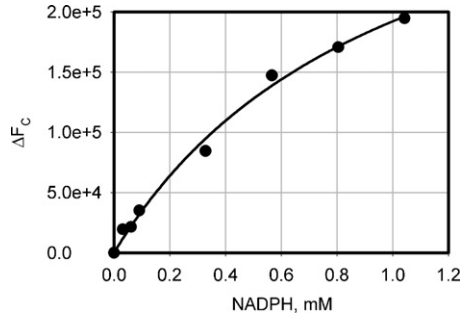

Fig. 4. Fluorescence titration with NADPH. The dots represent the measured change in emission (ΔF_c) and the line represents the predicted values obtained by fitting the experimental data to Eq. (6) by nonlinear regression analysis.

The steady-state ordered Bi Bi mechanism is common among nicotinamide nucleotide-dependent oxidoreductases and has also been proposed for the KR from the malaria parasite *P. falciparum* [19], for the related enoyl-ACP reductase from *Brassica napus* (rape) [27], and for other members of the SDR superfamily (e.g. [28–30]). Structural studies on the KR from *E. coli* provided evidence for considerable conformational changes after binding of the cofactor leading to the hypothesis of an ordered kinetic mechanism in which the binding of NADPH is an essential prerequisite for the binding of the keto substrate [16]. In contrast, rapid-equilibrium and steady-state random Bi Bi mechanisms were proposed for the KRs from *S. pneumoniae* [17] and *Mycobacterium tuberculosis* [18], respectively. The observed product inhibition patterns in this study eliminated the possibility of both random mechanisms. In the rapid-equilibrium random mechanism (without formation of dead-end complexes) all product inhibition patterns would be competitive and the steady-state random mechanism would result in non-competitive inhibition in case of all four substrate–product combinations [31].

From an application-oriented point of view, the presented results revealed that both reaction products caused only a weak inhibition of the cyanobacterial KR. High apparent inhibition constants in the range of 7–200 times the K_m of the corresponding substrate were observed. The enzyme showed a steep activity decrease at substrate and cofactor concentrations below 10 mM ECAA and/or 1 mM NADPH, respectively. To realize an economically feasible process involving the KR, a high NADPH concentration and an efficient *in situ* regeneration of the oxidized cofactors would be necessary. The application of an artificial fusion protein between the KR from *Synechococcus* sp. strain PCC 7942 and a cofactor regenerating enzyme has been shown to result in higher reaction rates than an equimolar mixture of the independent enzymes [32]. The identification of the reaction mechanism of the KR is a first step toward a deeper understanding of this finding and the modelling of the coupled enzymatic reaction.

5. Conclusion

In summary, the KR from the freshwater cyanobacterium *Synechococcus* sp. strain PCC 7942 has been shown to obey a steady-state ordered Bi Bi mechanism. The correct assignment of the kinetic mechanism is the fundamental basis for the mathematical description and optimization of large-scale KR-catalysed reduction reactions.

References

[1] M.C. Hogan, J. Woodley, Chem. Eng. Sci. 55 (2000) 2001–2008.
[2] T. Schmidt, C. Michalik, M. Zavrel, A. Spieß, W. Marquardt, M.B. Ansorge-Schumacher, Biotechnol. Prog. 26 (2010) 73–78.
[3] D.P.C. de Barros, F. Lemos, L.P. Fonseca, J.M.S. Cabral, J. Mol. Catal. B: Enzym. 66 (2010) 285–293.
[4] J.D. Stewart, Curr. Opin. Chem. Biol. 5 (2001) 120–129.
[5] K. Nakamura, R. Yamanaka, T. Matsuda, T. Harada, Tetrahedron: Asymmetry 14 (2003) 2659–2681.
[6] H.K. Chenault, G.M. Whitesides, Appl. Biochem. Biotechnol. 14 (1987) 147–197.
[7] W.A. van der Donk, H. Zhao, Curr. Opin. Biotechnol. 14 (2003) 421–426.
[8] R. Pereira, Crit. Rev. Biotechnol. 18 (1998) 25–64.
[9] H. Yamamoto, A. Matsuyama, Y. Kobayashi, Appl. Microbiol. Biotechnol. 61 (2003) 133–139.
[10] K. Hölsch, J. Havel, M. Haslbeck, D. Weuster-Botz, Appl. Environ. Microbiol. 74 (2008) 6697–6702.
[11] K. Hölsch, D. Weuster-Botz, Enzyme Microb. Technol. 47 (2010) 228–235.
[12] S.W. White, J. Zheng, Y.M. Zhang, C.O. Rock, Annu. Rev. Biochem. 74 (2005) 791–831.

[13] Q. Ren, N. Sierro, B. Witholt, B. Kessler, J. Bacteriol. 182 (2000) 2978–2981.
[14] H. Wright, Structure 12 (2004) 358–359.
[15] J.W. Campbell, J.E. Cronan Jr., Annu. Rev. Microbiol. 55 (2001) 305–332.
[16] A.C. Price, Y.M. Zhang, C.O. Rock, S.W. White, Biochemistry 40 (2001) 12772–12781.
[17] M.P. Patel, W.S. Liu, J. West, D. Tew, T.D. Meek, S.H. Thrall, Biochemistry 44 (2005) 16753–16765.
[18] R.G. Silva, L.P. de Carvalho, J.S. Blanchard, D.S. Santos, L.A. Basso, Biochemistry 45 (2006) 13064–13073.
[19] S.R. Wickramasinghe, K.A. Inglis, J.E. Urch, S. Müller, D.M.F. van Aalten, A.H. Fairlamb, Biochem. J. 393 (2006) 447–457.
[20] J. Heukeshoven, R. Dernick, Elektrophoresis 9 (1988) 28–32.
[21] S. Bräutigam, S. Bringer-Meyer, D. Weuster-Botz, Tetrahedron: Asymmetry 18 (2007) 1883–1887.
[22] J. Lakowicz, Principles of Fluorescence Spectroscopy, Springer, Berlin, 2006, pp. 63–67.
[23] C.C. Field, W.T. Birdsong, R.H. Goodman, Proc. Natl. Acad. Sci. U.S.A. 100 (2003) 9202–9207.
[24] W.W. Cleland, in: P.D. Boyer (Ed.), The Enzymes, vol. 2, 3rd ed., Academic Press, New York, 1970, pp. 1–65.
[25] J.T. Wu, L.H. Wu, J.A. Knight, Clin. Chem. 32 (1986) 314–319.
[26] S. Shimizu, M. Kataoka, M. Katoh, T. Morikawa, T. Miyoshi, H. Yamada, Appl. Environ. Microbiol. 56 (1990) 2374–2377.
[27] T. Fawcett, C.L. Copse, J.W. Simon, A.R. Slabas, FEBS Lett. 484 (2000) 65–68.
[28] B.A. Skalhegg, Eur. J. Biochem. 50 (1975) 603–609.
[29] B. Sahni-Arya, M.J. Flynn, L. Bergeron, M.E. Salyan, D.L. Pedicord, R. Golla, Z. Ma, H. Wang, R. Seethala, S.C. Wu, J.J. Li, A. Nayeem, C. Gates, L.G. Hamann, D.A. Gordon, Y. Blat, Biochim. Biophys. Acta 1774 (2007) 1184–1191.
[30] J. Stojan, M. Brunskole, T.L. Rižner, Chem. Biol. Interact. 178 (2009) 268–273.
[31] W.W. Cleland, Adv. Enzymol. Relat. Areas Mol. Biol. 45 (1977) 273–387.
[32] K. Hölsch, D. Weuster-Botz, Biotechnol. Appl. Biochem. 56 (2010) 131–140.